Macromolecular Rapid Communications
www.mrc-journal.de

Native Structure of the Plant Cell Wall Utilized for Top-Down Assembly of Aligned Cellulose Nanocrystals into Micrometer-Sized Nanoporous Particles

Panagiotis Spiliopoulos, Iina Solala, Timo Pääkkönen, Jani Seitsonen, Bas van Bochove, Jukka V. Seppälä, and Eero Kontturi**

Despite their sustainable appeal, biomass components are currently undervalued in nanotechnology because means to control the assembly of bio-based nanoparticles are lagging behind the synthetic counterparts. Here, micrometer-sized particles consisting of aligned cellulose nanocrystals (CNCs) are prepared by crosslinking cellulose in cotton linter fibers that are prehydrolyzed with gaseous HCl, resulting in chemical cleavage necessary for CNC formation but retaining the morphology of the native fibers. That way, the intrinsic alignment of cellulose microfibrils within the fiber cell wall can be retained and utilized for top-down CNC alignment. Subsequent crosslinking with citric acid cements the alignment and preserves it, following the dispersion of CNCs trapped end-to-end, connected, and crosslinked within the colloidally stable micrometer-sized particles. Furthermore, thermoporosimetry and cryogenic transmission electron microscopy (Cryo TEM) shows that the particles possess mainly nanoporous (<2 nm) character in water. The approach challenges the current paradigm of predominantly bottom-up methods for nanoparticle assembly.

Nanoparticle (NP) assembly has attracted widespread attention within the last decades owing to its numerous application possibilities in areas such as chemical catalysis,[1] sensory, optical devices,[2,3] and medicine.[4,5] In this realm, biologically derived nanoparticles enable the construction of ever more sophisticated assemblages,[6–11] either via direct self-assembly processes or through an external template.[12] Herein, we introduce an unprecedented approach for template-driven top-down assembly of cellulose nanocrystals (CNCs): Covalent crosslinking of the nanocrystals, while still trapped in their native environment of the plant cell wall. The resulting colloidally stable, micrometer-sized, porous particles consist of CNCs that are perfectly aligned with each other. The structures represent a conceptually new way of utilizing a biosynthetically derived mold for manipulating nanoparticles.

Cellulose—the main structural constituent of the plant cell wall—is organized in microfibrils which exhibit parallel alignment with respect to each other. In fact, plenty of the advanced properties of plant-based fibers originate from this scaffold-like structure.[13,14] The microfibrils themselves are semicrystalline[15] and their crystalline regions can be isolated as CNCs: rod-shaped particles of 5–30 nm in diameter and 50–1000 nm in length, depending on their native source.[16] CNCs are chiral and exceptionally strong mechanically, resulting in plenty of advantages considering applications such as high-end composites,[16–21] chiral supports,[22–27] and energy storage.[28] Besides, they are bio-based and biodegradable. Most isolation ways for CNCs rely on harsh acidic, liquid/solid reaction systems, ending up with sulfate-charged, water-dispersible CNCs that have completely repudiated their native orientation.[29] CNC assembly has been extensively studied, mainly focusing on the formation of chiral nematic liquid crystals[30] as well as alignment[24,31] by utilizing, e.g., an external magnetic field,[32] confined geometry,[31] or high shear.[33–35] Furthermore, Way et al.[36] have described the formation of pH stimulated CNC assemblies, while covalent crosslinking of arbitrarily associated CNCs has also been reported.[37,38] The stimuli responsive approaches for bottom-up alignment of CNCs were recently reviewed.[39] However, all prementioned techniques for CNC assembly involve bottom-up processes. Our top-down approach involves covalent crosslinking of CNCs before their dispersion, in the native template of the secondary cell wall, retaining and utilizing their initial biosynthetic alignment. To achieve that, we have exploited our newly introduced method,[40,41] namely HCl

P. Spiliopoulos, Dr. I. Solala, Dr. T. Pääkkönen, Prof. E. Kontturi
Department of Bioproducts and Biosystems
Aalto University
P. O. Box 16300, Espoo FI-00076, Finland
E-mail: iina.solala@aalto.fi; eero.kontturi@aalto.fi
Dr. J. Seitsonen
Department of Applied Physics
Aalto University
P. O. Box 15100, Espoo FI-00076, Finland
Dr. B. van Bochove, Prof. J. V. Seppälä
Department of Chemical and Metallurgical Engineering
Aalto University
P. O. Box 16300, Espoo FI-00076, Finland
The ORCID identification number(s) for the author(s) of this article can be found under https://doi.org/10.1002/marc.202000201.

DOI: 10.1002/marc.202000201

Macromolecular Rapid Communications
www.mrc-journal.de

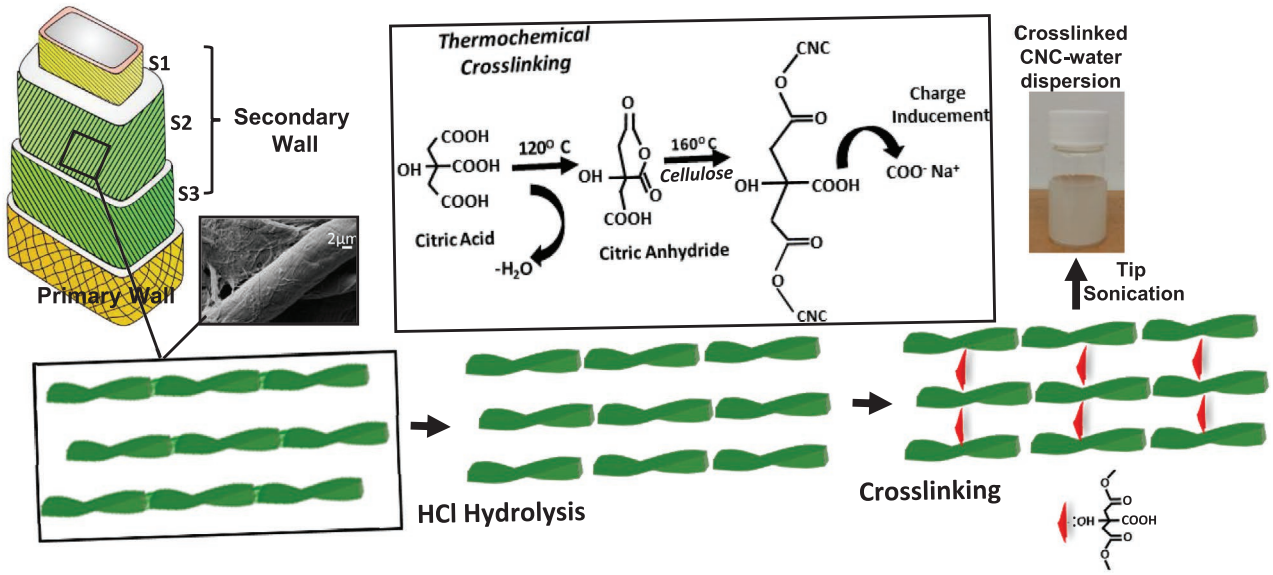

Figure 1. Fiber hydrolysis and thermochemical crosslinking mechanism. Citric acid turns to the anhydride form via heating at 120 °C and is further esterified with two cellulosic hydroxyls at 160 °C. Charge inducement on the remaining nonesterified carboxylic groups through NaOH exposure leads to stable CNC dispersion in water.

gas hydrolysis in a gas/solid system. It is a process where the fiber morphology and the microfibril orientation remain intact, yet the fibers have been hydrolyzed down to level-off degree of polymerization (LODP), signifying that all dislocations between the crystalline segments in microfibrils have been degraded. This implies, in essence, that the hydrolyzed fibers consist of end-to-end connected, oriented CNCs. Subsequently, we have crosslinked the oriented CNCs by simple esterification with a tricarboxylic acid[42]—before dispersing the CNCs into an aqueous medium as crosslinked particles.

The experimental set-up is illustrated schematically in **Figure 1** and described in detail in the Supporting Information. Whatman 1 filter paper from cotton linter fibers was used as a cellulose source that was hydrolyzed down to the LODP by HCl gas. Esterification with citric acid (CA) was undertaken directly afterward, followed by a mild 0.1 M NaOH treatment for ionizing the free (nonesterified) COOH groups of the CA crosslinkers. This produced aligned CNCs trapped in microsized particles that formed a stable colloidal dispersion upon sonication. We stress that the HCl hydrolysis had to be performed before crosslinking as the ester linkages by CA were predominantly cleaved due to ester hydrolysis by catalyzed by HCl if the sequence was performed in reverse order, i.e., CA crosslinking before HCl hydrolysis (Figure S7, Supporting Information).

The size and shape of the dispersed particles was characterized by atomic force (AFM) and transmission electron microscopies (TEM) revealing that hydrolyzed fiber segments were indeed crosslinked in an aligned manner (**Figure 2**a–d; Figure S3, Supporting Information). The images reveal particles of 1.5 μm average length (as opposed to 100–300 nm, characteristic of CNCs[16,43]). These particles actually consist of multiple individual CNCs, as witnessed by the reduction in the molecular weight distribution down to the LODP (Figure S2, Supporting Information), indicating that only cellulose crystallites are left within the treated fibers.[40] Increased magnification images (Figure 2b,d) reveal good alignment of the nanocrystals in the crosslinked structure, similar to the one exhibited within microfibrils along the secondary plant cell wall.[44] Thus, thermochemical crosslinking did not interfere with the native order, leading to the formation of a 3D network of CNCs, aligned according to the native fibrillar orientation of the secondary cell wall (see Figure 1 for schematics). It is clear from Figure 2 that the degree of alignment is very high compared with most previous accounts,[32,45] although it is confined to micrometer-sized particles. Another intriguing feature is that the CNCs, as they stand in the fiber-like aggregates (Figure 2), must be end-to-end connected with each other, simply because the microfibril morphology of the original fibers has not been broken although the chemical cleavage down to CNC level is apparent from the GPC data (Figure S2, Supporting Information). This end-to-end connection is likely not covalent crosslinking between adjacent CNCs but a result of the integrity of the aggregate which retains the microfibrillar morphology of the original secondary wall.

To obtain a better overview of the particle sizes, fractionation was carried out by centrifugation and the resulting fractions were examined by AFM (Figure 2e–f) and optical microscopy (Figure S4, Supporting Information). Centrifugation leads to an efficient separation of the crosslinked, bigger particles (3–5 μm in length) from the fine fraction of smaller particles or even isolated CNCs (<1 μm) as shown in Figure 2e,f respectively, in good agreement with the optical microscopy images. Finally, we tested whether the crosslinked complexes could be disrupted into their constituent CNCs through saponification by strong alkali (25% NH_4OH), a process where the hydroxide ion cleaves the ester bond of the CA. **Figure 3**b shows how isolated CNCs with their familiar rod-like shapes and dimensions (mostly 100–300 nm length, 5–20 nm width, concurrent with literature values[46]) can be distinguished after the saponification and exposure to liquid water.

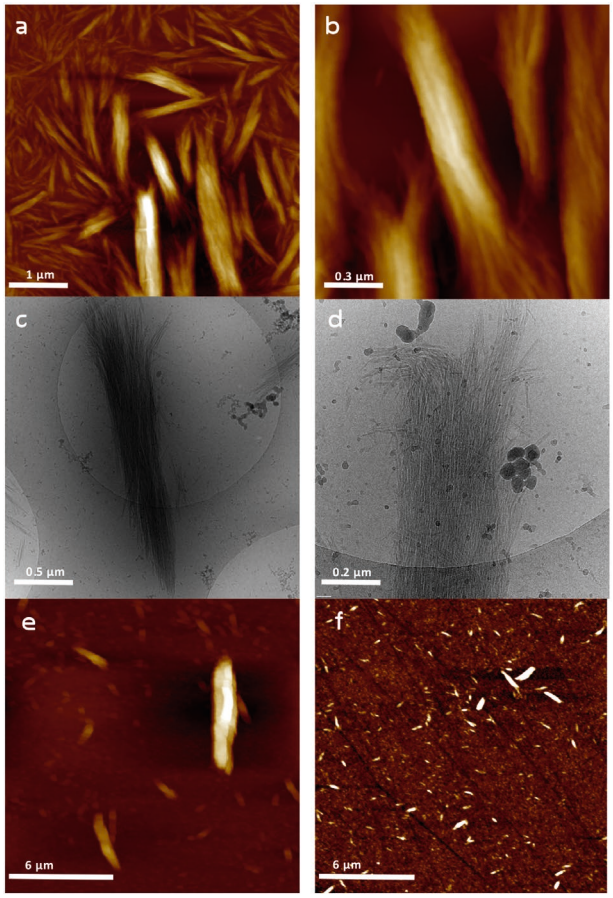

Figure 2. a,b) AFM and c,d) TEM images of crosslinked CNCs before fractionation; e) sediment and f) supernatant phases of the centrifuged crosslinked sample.

As for the characterization, photoacoustic Fourier transform infrared (FTIR) measurements demonstrated efficient thermochemical crosslinking formation (esterification), as well as charge incorporation in the crosslinked complex (Figure 3a). First, the crosslinking, as illustrated in Figure 1, is indicated by the emerging carbonyl contribution (1735 cm^{-1}) in Figure 3a. Mild alkaline treatment was then applied to distinguish the charged carboxylic contribution (1580 cm^{-1}) from the ester crosslinks (1735 cm^{-1}) (Figure 3a). The esters emerge from reacted CA whereas the carboxylates emerge from unreacted CA (see, Figure 1).

Conductometric titration (Figure S1, Supporting Information) showed the presence of 0.72 mmol g^{-1} carboxylate content within the crosslinked structures. This represents high charge density, comparable in the order of magnitude to, e.g., the values introduced by (2,2,6,6-tetramethylpiperidine-1-oxyl radical)-mediated oxidation of cellulose microfibrils (often 1.0–2.0 mmol g^{-1}).[47] It is sufficient to grant electrostatic stabilization in the dispersion (Figure 1). We emphasize that all charge contribution arises from unreacted carboxyls (Figure 1) in the crosslinking CA.

The pore size distribution (PSD) of the crosslinked structures was determined by thermoporosimetry (**Figure 4**a). We emphasize that thermoporosimetry enables the measure of PSD in water, utilizing the melting point depression inside nanosized pores via the Gibbs-Thomson correlation. Figure 4 shows how the crosslinking manages to preserve the PSD of the cell wall as the differences before and after were minute. The majority of pore volume arises from the nanoporous (≈2 nm) gaps between the CNCs within the structures. The cryogenic transmission electron microscopy (Cryo TEM) images (Figure 4b) taken directly from the vitrified dispersions agree with the PSD results: ≈2 nm pores are visible between the aligned and crosslinked CNCs. Otherwise, most of the larger pores are in the mesoporous scale (2–50 nm). Such PSD is unusual with cellulosic fibers as in most cases, the PSD is represented by an inverse pattern where macropores at ≈100 nm diameter form the majority of the pore volume.[48] The high volume of nanopores in the hydrolyzed samples is likely the result of HCl (g) hydrolysis, which leads to additional

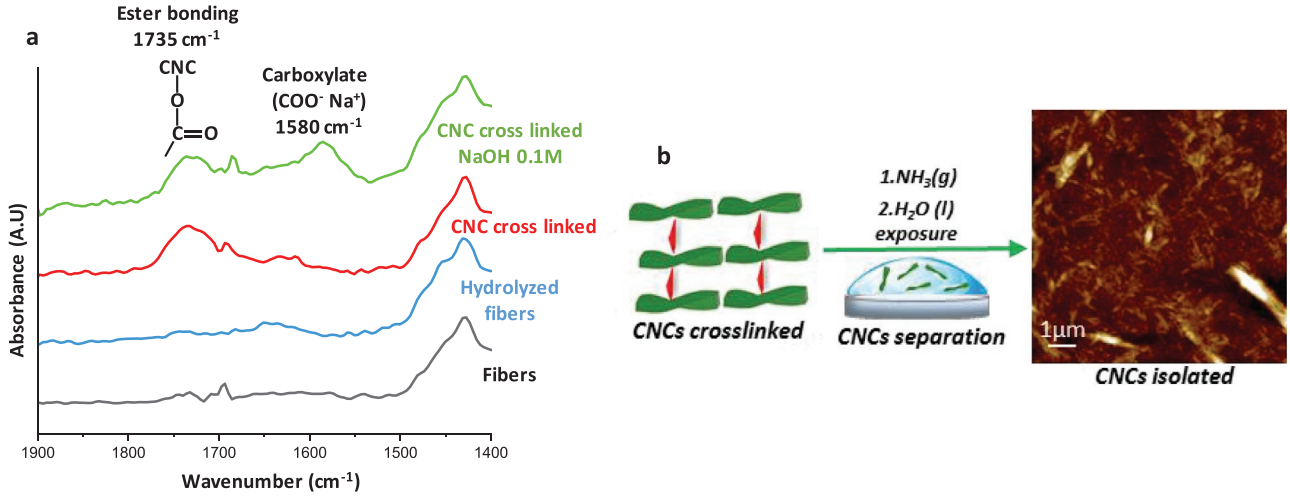

Figure 3. a) Photoacoustic FTIR spectra of cotton linter fibers before and after hydrolysis, crosslinked CNC as well as crosslinked and NaOH treated CNC. NaOH treatment induces a new band due to carboxylate formation on the nonesterified carboxylic acid, compensating for the surface area reduction of the ester bonding band. b) Crosslinked hydrolyzed fibers separation through saponification and exposure to liquid water. NH_4OH cleaves the ester bonding between the nanocrystals, while drop-casting of water droplet separates them upon evaporation.

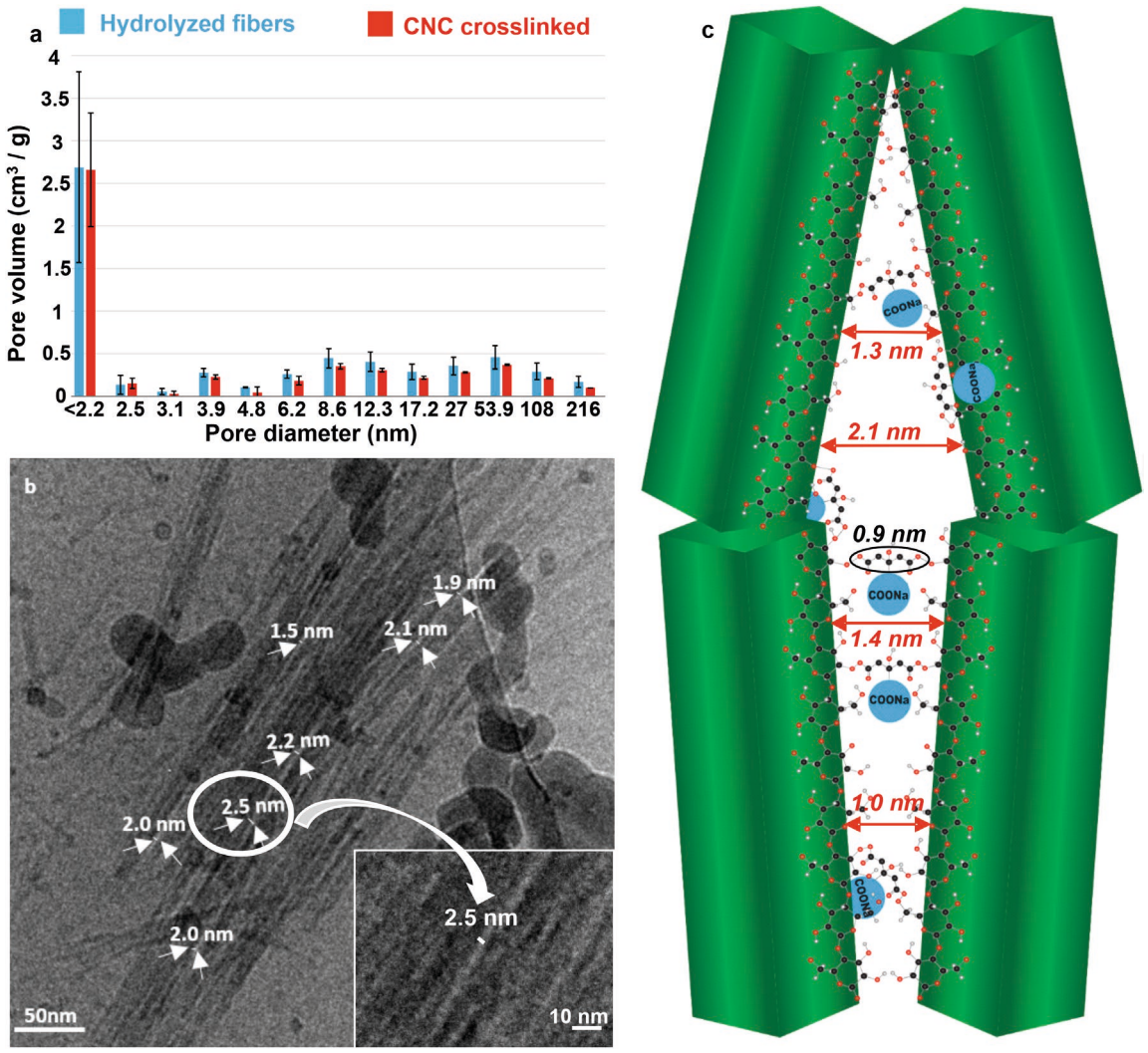

Figure 4. a) Pore size distribution of hydrolyzed fiber and CNC crosslinked sample. b) TEM image of the CNC crosslinked sample. c) Schematic representation of the crosslinked nanocrystals, interparticle distance and network porosity (the dimensions are not to scale).

crystallization of cellulose.[40,49] Overall, the cumulative pore volume (porosity) of the crosslinked aggregates is 5.15 $cm^3\ g^{-1}$ (see the cumulative distributions in Figure S8 in the Supporting Information).

Chemical and physical characterization enables us to draw a quantitative picture of the crosslinked CNCs (see Figures S5 and S6, and calculations in Section S2.6 in the Supporting Information). FTIR data was quantified by using a benzyl acetate calibration series, revealing that the ester content in the crosslinked fibers was 0.9 ± 0.2 mmol g^{-1}. Because conductometric titration gave a charge density of 0.7 mmol g^{-1}, the apparent ratio of esters to free carboxylates was 9/7 (1.3) whereas the theoretical ratio is 2/1 (2.0) as two of the three carboxylates in each CA molecule are capable of esterification via the anhydride intermediate (Figure 1). Thus, the crosslinking was extensive but it did not reach its full potential. Furthermore, the crosslinking by CA is not likely to always occur between adjacent CNCs; it may also occur within the same CNC between neighboring anhydroglucose units (Figure 4c).

Our calculations show, nevertheless, that ≈50% of the anhydroglucose units on the CNC surfaces bear an ester bond. The porosity measurements (Figure 4) also demonstrate that the crosslinking between adjacent CNCs is substantial enough to resist additional swelling due to increased charge, amounting to higher osmotic pressure inside the particle. As a result, crosslinking manages to preserve the largely nanoporous (>2 nm) character of the hydrolyzed fibers, preventing extensive disintegration by sonication (Figure 4a,b).

In summary, a top-down CNC crosslinking technique using CA on cellulose fibers hydrolyzed by HCl gas was presented. Simultaneous crosslinking and charge introduction was achieved on CNCs, while maintaining their initial cell wall alignment. This resulted in micrometer-sized longitudinal particles with internal nanoporosity and good colloidal stability. As a result of their initial alignment and orientation, the crosslinked structures exhibited a well-defined continuous porous network, distinct from previously reported CNC structures. CNC alignment and nanoporosity was achieved by

utilizing the intrinsic native morphology of the fiber cell wall and it represents a conceptually new approach to preparing assemblies of nanoparticles derived from biomass components. The resulting particles may find use in, e.g., pharmaceutical, analytical, or capturing applications.

Supporting Information

Supporting Information is available from the Wiley Online Library or from the author.

Acknowledgements

Academy of Finland (300364) is acknowledged for the financial support. E.K. is grateful for the support by the FinnCERES Materials Bioeconomy Ecosystem.

Conflict of Interest

The authors declare no conflict of interest.

Keywords

hydrolysis, nanocellulose, porous materials, templated assembly

Received: April 14, 2020
Revised: June 17, 2020
Published online: July 1, 2020

[1] M. Daniel, D. Astruc, *Chem. Rev.* **2004**, *104*, 293.
[2] D. V. Talapin, J. S. Lee, M. Kovalenko, E. Schevckenko, *Chem. Rev.* **2010**, *110*, 389.
[3] E. Kontturi, P. Laaksonen, M. Linder, Nonappa, H. A. Gröschel, O. J. Rojas, O. Ikkala, *Adv. Mater.* **2018**, *30*, 1703779.
[4] R. Pugliese, F. Gelain, *Trends Biotechnol.* **2017**, *35*, 145.
[5] A. Chinen, C. M. Guan, J. R. Ferrer, S. N. Barnaby, J. T. Merkel, C. A. Mirkin, *Chem. Rev.* **2015**, *115*, 10530.
[6] Q. Yu, X. Zhang, Z. Zhang, R. Wang, *Nano Lett.* **2016**, *10*, 7485.
[7] P. Singh, Y. J. Kim, D. Zhang, D. C. Yang, *Trends Biotechnol.* **2016**, *34*, 588.
[8] H. Lee, J. Rho, P. B. Messersmith, *Adv. Mater.* **2009**, *21*, 431.
[9] S. V. Patwardhan, C. C. Perry, *J. Mater. Chem.* **2007**, *17*, 2875.
[10] I. Ocsoy, D. Tasdemir, S. Mazicioglu, C. Celik, A. Kati, F. Ulgen, *RSC Adv.* **2018**, *8*, 25298.
[11] C. Jia, B. Luo, H. Wang, Y. Bian, X. Li, S. Li, H. Wang, *Adv. Mater.* **2017**, *29*, 1701154.
[12] M. Grzelczak, J. Vermant, E. M. Furst, L. Liz-Marzán, *Nano Lett.* **2010**, *4*, 3591.
[13] J. Sugiyama, H. Chanzy, G. Maret, *Macromolecules* **1992**, *25*, 4232.
[14] T. I. Baskin, *Protoplasma* **2001**, *215*, 150.
[15] B. J. Hidayat, C. Felby, K. S. Johansen, L. G. Thygesen, *Cellulose* **2012**, *19*, 1481.
[16] J. George, S. N. Sabapathi, *Nanotechnol. Sci. Appl.* **2015**, *8*, 45.
[17] J. R. McKee, J. Huokuna, L. Martikainen, M. Karesoja, A. Nykänen, E. Kontturi, H. Tenhu, J. Ruokolainen, O. Ikkala, *Angew. Chem. Int. Ed.* **2014**, *53*, 5049.
[18] H. Liu, D. Liu, F. Yao, Q. Wu, *Bioresour. Technol.* **2010**, *101*, 5685.
[19] X. Qin, W. Xia, R. Sinko, S. Keten, *Nano Lett.* **2015**, *15*, 6738.
[20] C. E. Boott, A. Tran, W. Y. Hamad, M. J. MacLachlan, *Angew. Chem., Int. Ed.* **2020**, *59*, 226.
[21] F. Ansari, L. A. Berglund, *Biomacromolecules* **2018**, *19*, 2341.
[22] C. C. Cheung, M. Giese, J. A. Kelly, W. Y. Hamad, M. J. MacLachlan, *ACS Macro Lett.* **2013**, *2*, 1016.
[23] J. A. Kelly, M. Giese, K. E. Shopsowitz, W. H. Hamad, M. J. MacLahlan, *Acc. Chem. Res.* **2014**, *47*, 1088.
[24] V. Cherpak, V. Korolovych, R. Geryak, T. Turiv, D. Nepal, J. Kelly, T. Bunning, O. Lavrentovich, W. Heller, V. Tsukruk, *Nano Lett.* **2018**, *18*, 6770.
[25] J. Majoinen, J. Hassinen, J. S. Haataja, H. T. Rekola, E. Kontturi, M. A. Kostiainen, R. H. Ras, P. Törmä, O. Ikkala, *Adv. Mater.* **2016**, *28*, 5262.
[26] O. Lidor-Shalev, N. Pliatsikas, Y. Carmiel, P. Patsalas, Y. Mastai, *Nano Lett.* **2017**, *11*, 4753.
[27] R. M. Parker, G. Guidetti, C. A. Williams, T. Zhao, A. Narkevicius, S. Vignolini, B. Frka-Petesic, *Adv. Mater.* **2018**, *30*, 1704477.
[28] Z. Xu, F. Xie, J. Wang, H. Au, M. Tebyetekerwa, Z. Guo, S. Yang, Y. Hu, M. Titirici, *Adv. Funct. Mater.* **2019**, *29*, 1903895.
[29] J. J. Hebert, J. H. Carra, C. R. Esposito, M. L. Rollins, *Text. Res. J.* **1973**, *43*, 260.
[30] J. P Lagerwall, C. Schütz, M. Salajkova, J. Noh, J. H. Park, G. Scalia, Bergström, *NPG Asia Mater.* **2014**, *6*, e80.
[31] R. M. Parker, B. Frka-Petesic, G. Guidetti, G. Kamita, G. Consani, C. Abell, S. Vignolini, *Nano Lett.* **2016**, *10*, 8443.
[32] K. J. De France, K. G. Yager, T. Hoare, E. D. Cranston, *Langmuir* **2016**, *32*, 7564.
[33] D. Liu, X. Chen, Y. Yue, M. Chen, Q. Wu, *Carbohydr. Polym.* **2011**, *84*, 316.
[34] M. K. Hausmann, P. A. Ruhs, G. Siqueira, J. Läuger, R. Libanori, T. Zimmermann, A. R. Studart, *Nano Lett.* **2018**, *12*, 6926.
[35] I. Hoeger, O. J. Rojas, K. Efimenko, O. D. Velev, S. S. Kelley, *Soft Matter* **2011**, *7*, 1957.
[36] A. E. Way, L. Hsu, K. Shanmuganathan, C. Weder, S. J. Rowan, *ACS Macro Lett.* **2012**, *1*, 1001.
[37] X. Yang, E. D. Cranston, *Chem. Mater.* **2014**, *26*, 6016.
[38] L. Goetz, A. Mathew, K. Oksman, P. Gatenholm, A. J. Ragauskas, *Carbohydr. Polym.* **2009**, *75*, 85.
[39] Q. Zhu, Q. Yao, J. Sun, H. Chen, W. Xu, J. Liu, Q. Wang, *Carbohydr. Polym.* **2020**, *230*, 115609.
[40] E. Kontturi, A. Meriluoto, P. A. Pentillä, N. Baccile, J. M. Malho, A. Potthast, T. Rosenau, J. Ruokolainen, R. Serimaa, J. Laine, H. Sixta, *Angew. Chem., Int. Ed.* **2016**, *55*, 14455.
[41] T. Pääkkönen, P. Spiliopoulos, A. Knuts, K. Nieminen, L. Johansson, E. Enqvist, E. Kontturi, *React. Chem. Eng.* **2018**, *3*, 312.
[42] C. Demitri, R. Del Sole, F. Scalera, A. Sannino, G. Vasapollo, A. Maffezzoli, L. Ambrosio, L. Nicolais, *J. Appl. Polym. Sci.* **2008**, *110*, 2453.
[43] R. R. Lahiji, X. Xu, R. Reifenberger, A. Raman, A. Rudie, R. J. Moon, *Langmuir* **2010**, *26*, 4480.
[44] H. Yu, R. Liu, D. Shen, Y. Jiang, Y. Huang, *Polymer* **2005**, *46*, 5689.
[45] Y. Habibi, T. Heim, R. Douillard, *J. Polym. Sci., Part B: Polym. Phys.* **2008**, *46*, 1430.
[46] Y. Habibi, L. A. Lucia, O. J Rojas, *Chem. Rev.* **2010**, *110*, 3479.
[47] R. Salminen, M. Reza, T. Pääkkönen, J. Peyre, E. Kontturi, *Cellulose* **2017**, *24*, 1657.
[48] R. Salminen, M. Reza, K. Vanhatalo, E. Kontturi, *Cellulose* **2017**, *24*, 5697.
[49] T. Pääkkönen, P. Spiliopoulos, D. Nonappa, K. S. Kontturi, P. Penttilä, M. Viljanen, K. Svedström, E. Kontturi, *ACS Sustainable Chem. Eng.* **2019**, *7*, 14384.